Recombination mechanisms in highly doped CdS:In

Ch. Fricke, R. Heitz, A. Hoffmann, and I. Broser
Institut fuer Festkoerperphysik, Technische Universitaet Berlin, Hardenbergstrasse 36, 10623 Berlin, Germany
(Received 27 August 1993)

Time-resolved luminescence measurements of CdS:In crystals in the near-band-gap region are presented for a wide range of indium doping levels, i.e., for concentrations between 10^{17} and 10^{20} cm^{-3}. Interactions of the indium dopants lead to a broad luminescence band near the band-gap energy and alter the luminescence dynamics. A decrease of the lifetimes of both donor and acceptor bound exciton complexes is observed at medium doping levels (10^{17}–10^{18} cm^{-3}). This is explained by the reduction of the effective binding energies leading to shorter decay constants of these complexes. The decay of the donor-acceptor-pair recombination luminescence is also investigated for indium concentrations below the Mott density. A statistical model proposed by Thomas and Hopfield is used to determine the electronically active impurity concentration. At higher doping levels (up to 10^{20} cm^{-3}) the degeneracy of the conduction band leads to a luminescence band attributed to radiative non-k-conserving band-to-band transitions. The measured lifetimes reflect the number of occupied states in the conduction band and the number of free states in the valence band. A nonexponential fit reveals the concentration of electronically active impurity centers. A correlation between photogenerated and doping-generated carriers is established for high excitation densities.

I. INTRODUCTION

Wide-band-gap II-VI materials became of extreme interest since the reproducible fabrication of highly p-doped epitaxial structures has been realized recently. Based on these materials, new prospects are opened for technical applications such as short-wavelength lasers[1] and detectors. However, the most efficient application of fast nonlinear emission, transmission, or reflectivity switching processes requires a detailed knowledge on the physics of heavily p- or n-type-doped II-VI compounds. To clear up these problems thorough studies on the linear and nonlinear optical properties and, in particular, on the dynamics in these materials are necessary. Up to now, only a little information about the influence of high doping concentrations on the electronic processes of semiconductors existed. One of the first materials which has been investigated in the highly doped regime was CdS:Cl. With increasing chlorine doping concentration a strong broadening of the excitonic structures and the luminescence of the donor-acceptor-pair (DAP) recombination is observed.[2,3,4] The broadening is explained by a decrease of the binding energy of the bound exciton complex. Hanamura calculated the screening of the Coulomb interaction due to localized donor electrons.[5] The screening decreases the bound and free exciton binding energy and thus increases the I_2 emission energy. Additional information on the optical properties of highly doped semiconductors is obtained from studies of the donor-acceptor-pair recombination luminescence. Colbow[6] has discussed the decay in a model for exciton recombination giving a lower limit of 2.4 ns for the recombination time. Thomas *et al.*[7] performed time-integrated and time-resolved measurements showing a reduction of the decay time with increasing doping concentration and explained the development in a statistical approach by the reduction of the mean distance between donor and acceptor ions. The interaction between the host material and the dopants drastically changes the optical properties of the semiconductor. Doping concentrations above the Mott density lead to a degenerated semiconductor, i.e., the transition from the semiconducting to the metallic phase is observed.[8] Now non-k-conserving band-to-band transitions are the origin of the blue near-band-gap luminescence. According to the model of Kane,[9] the conduction band degenerates. The density of states extends significantly below the undisturbed conduction-band energy and the Fermi level increases. Recently, comprehensive works on CdS:In concerning the drastic changes in conduction and emission[10,11,12] with growing indium concentration have been published. Preliminary studies on the dynamical behavior of the near-band-gap luminescence[13] have been published.

In the present paper, more detailed and quantitative work on the dynamics of heavily doped CdS:In is presented. The explanation of the radiative recombination dynamics yields an understanding of the involved electronic recombination mechanisms as well as their dependence on impurity concentration and excitation density. Time-resolved luminescence measurements are introduced as a standard technique to determine the impurity concentration in II-VI semiconductors (bulk material as well as epilayers) for a wide range of concentrations. We will demonstrate that, in dependence on the doping concentrations, three main photoluminescence processes influence the dynamics: the donor-acceptor-pair luminescence (part I in Fig. 1), the bound exciton recombination (part II in Fig. 1), and the band-to-band transition (part III in Fig. 1).

II. EXPERIMENTAL TECHNIQUE

The investigated CdS crystals are grown by the Frerichs-Warminsky method from the gaseous phase.[14]

The indium doping for the highest doping levels was achieved during growth and the concentrations are deduced by atomic absorption spectroscopy. Smaller indium concentrations were realized by covering selected undoped CdS crystals with indium. The average thickness of the indium layers varied between 2 and 200 nm; the number of doping atoms at the crystal surface was therefore 10^{13}–10^{16} cm^{-2}. Subsequently, the crystals were annealed for 20 h in vacuum at a temperature of 900 °C. The doping concentration is calculated assuming that all indium has diffused into the crystal. For the luminescence measurements the crystals are immersed in liquid He at 2 K. A synchronously pumped dye laser with 3 ps pulse duration and 1.9 MHz repetition rate excites the samples with a maximum average output power of 100 mW at 2.65 eV. Coumarin 120 is used as dye permitting a tuning range in the blue-green spectral range (440–485 nm). The intensity is varied by neutral glass filters for low excitation densities. Time-resolved luminescence measurements are performed with a subtractive grating monochromator and a microchannel plate (MCP) photomultiplier tube (PMT) using time-correlated single photon counting. A resolution better than 10 ps for rise and decay times is achieved by numerical deconvolution of the luminescence transients with the apparatus response.

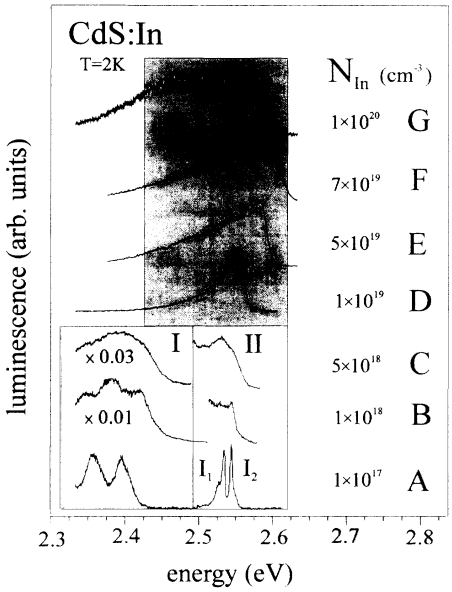

FIG. 1. Luminescence spectra for CdS:In crystals in dependence on the indium concentration for low excitation densities (I_{exc}=10 kW cm^{-2}). Indium concentrations are deduced from growth conditions. The letters *A*–*G*, attributed to each curve, are used for all the figures.

III. EXPERIMENTAL RESULTS

A. Time-integrated luminescence

Figure 1 shows time-integrated luminescence spectra at liquid helium temperature of CdS crystals doped with indium at concentrations (N_{In}) between 10^{17} and 10^{20} cm^{-3}. The lowest spectrum in Fig. 1 exhibits, in the near-band-gap region (region II in Fig. 1), two luminescence lines I_1, the radiative recombination of an exciton bound to a neutral acceptor, and I_2, the corresponding recombination of an exciton bound to a neutral donor. The energy position of the I_2 line at 2.5460 eV corresponds to a bound exciton complex formed at a substitutional indium impurity on cadmium site.[15] Interactions between the impurity centers as well as the statistical distribution of doping atoms throughout the sample influence the linewidths of all radiative decays. Even indium concentrations around 10^{17} cm^{-3} influence this luminescence significantly; the linewidth is increased to 5 meV. Shifts of several meV towards higher energies of the exciton luminescence lines with increasing donor concentration according to the theory of Hanamura mentioned above are not observed in our samples for doping levels below 5×10^{18} cm^{-3}.

The development of the DAP recombination (region I in Fig. 1) with increasing indium doping is similar to that of the excitonic structures. The strong dependence of the transition probability on the localization of electrons to a specific donor, on one hand, and variations of donor binding energy due to impurity-impurity interactions, on the other hand, lead to broader luminescence structures. A characteristic density, the Mott density, is reached when the average distance between neighboring impurity centers, i.e., indium atoms, is comparable to or smaller than the Bohr radius (a_0^{In} = 2.4 nm). Theoretical calculations for CdS yield a density of $N_{Mott}=1.6\times10^{18}$ cm^{-3}, but experimental results[8,16–18] demonstrate that it is reached for $N_{In}=5\times10^{18}$ cm^{-3}. Above that density donors and acceptors are ionized and consequently the DAP recombination luminescence is no longer observed. At the Mott density a phase transition takes place. The donor states degenerate with conduction-band states due to the screening of the Coulomb interaction. Instead of excitonic and DAP recombination luminescence, now non-*k*-conserving band-to-band transitions are observed.

CdS crystals with indium concentrations around $N_{In}=1\times10^{19}$ cm^{-3} and higher emit a broad asymmetric luminescence band around the band-gap energy (region III in Fig. 1). For the highest indium concentration (1×10^{20} cm^{-3}) the high energy edge of the observed luminescence band is observed at 2.612 eV at 2 K.[12,19] This is about 30 meV above the fundamental band gap of undoped CdS. The shape of this luminescence band results from the convolution of the density of occupied states in the conduction band and of the density of empty states in the valence band. Taking in addition the one-particle interaction and correlation energy into account, the luminescence band can be fitted as a function of N_D and N_A. Though this model gives a qualitative understanding of the luminescence of degenerated semiconductors, the values for the doping concentrations obtained[20] give only the order of magnitude.

Figure 1 demonstrates that the time-integrated luminescence sensitively reacts to changes in the doping back-

ground. However, a quantitative understanding is quite difficult. As will be shown in the following, the recombination dynamics of the different luminescence processes also are a function of N_{In}. A theoretical treatment of the radiative dynamics is by far more reliable than line shape analyses, since in the latter too many parameters are involved.

B. Time-resolved measurements

1. *The donor-acceptor-pair luminescence (region I)*

A green luminescence is observed around 2.38 eV at T=2 K in undoped CdS crystals and is attributed to donor-acceptor-pair recombination or to conduction-band–acceptor recombination.[21] Each donor-acceptor pair has a distinct separation r and a radiative recombination energy $E = E(r)$. We assume therefore exponential recombination kinetics for a single donor-acceptor pair. The superposition of a large number of exponential decays from each pair leads to the observed luminescence. Decay times in the range of ms to μs for the green luminescence are reported for undoped CdS samples. The total light decay is in principal similar to the case of GaP, a model substance for investigations of the DAP luminescence.[22]

The influence of doping on the DAP recombination dynamics is studied by time-resolved measurements. Figure 2 gives transients for crystals with indium concentrations below the Mott density, since the DAP luminescence is only visible in this concentration range. A simple qualitative measure for the influence of the indium concentration on the recombination dynamics is given by exponential fits of the early parts of the transients of the green luminescence. We observe in this model a reduction of the decay constants from 200–300 ns at $N_{In}= 1\times10^{17}$ cm^{-3} (curve A of Fig. 1) down to 10–20 ns at $N_{In}= 5\times10^{18}$ cm^{-3} (curve C of Fig. 1). Though the shape of the luminescence band as well as its spectral position (around 2.38 eV) are hardly influenced, the recombination times are significantly shorter compared to values taken from the literature.[7] A better description of the decay of the green luminescence is proposed in the following.

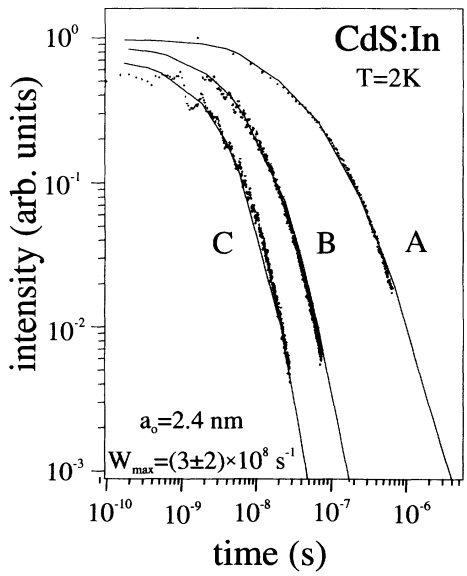

FIG. 2. Transients of the DAP luminescence in CdS with various N_{In} at low excitation densities ($I_{exc}= 10$ kW cm^{-2}). Points represent experimental data and the full lines give the theoretical fit using Eq. (2).

Using effective-mass approximation to calculate the recombination probability $W(r)$ for a single donor-acceptor pair, where one of the impurities has a significant smaller binding energy than the other, one gets

$$W(r) = W_{max} \exp\left[-\frac{2r}{a_0}\right] . \quad (1)$$

Equation (1) is only valid for pairs of reasonably large separation, i.e., $r \gg a_0$ (a_0 is the Bohr radius).[7] Due to the fact that only the Bohr radius of the weaker bound impurity atom is used to deduce Eq. (1), the following calculations are valid with the same Bohr radius a_0 for both acceptor or donor excess.

Admitting only hydrogenlike donors (valid for most of the group III donors in II-VI semiconductors) and donors or acceptors in excess, one gets for the intensity of light I emitted at time t (Ref. 7)

$$I(t) = \left\{4\pi N_D \int_0^\infty W(r) \exp\left[-W(r)t\right] r^2 dr\right\} \times \left\{\exp\left[4\pi N_D \int_0^\infty \left\{\exp\left[-W(r)t\right] - 1\right\} r^2 dr\right]\right\} . \quad (2)$$

N_D is the concentration of the majority constituent which should be of the order of the carrier concentration derived in Hall measurements at $T = 300$ K. Since the integral expressions are independent of N_D the logarithm of the observed luminescence intensity is a linear function of the impurity concentration N_D for a given W_{max} and a_0. Therefore, shorter decay times are expected with increasing N_D, a fact which is confirmed by the experiments showing faster recombination dynamics at higher doping concentrations.

Good agreement between theoretical calculations using Eq. (2) and experimental transients could be established (Fig. 2). The value of a_0 taken in the fits is the literature value for the InCd impurity center.[15] The fitting of the experimental data with a_0=2.4 nm and $W_{max}= (3\pm2)\times10^8$ s^{-1} using Eq. (2) gives the concentration of donors N_D in the CdS:In samples. Variations of 10% of the concentration N_D drastically influence the calculated decay behavior. Therefore, this theory allows us to fit precisely the number of impurity centers in the sample. As can be seen from Table I, the values N_D correspond reasonably well to those N_{In} deduced during the growth of the CdS:In crystals.

The dynamics of the DAP recombination in totally compensated crystals (N_D=N_A) with a doping concentration $N_D < N_{Mott}$ changes drastically. The statistical treatement of the DAP recombination dynamics is only valid for effective-mass-like impurity states, i.e., interactions with neighboring impurity centers should not

TABLE I. Fitted values according Eq. (2) for crystals $A - C$ (see Fig. 1).

Crystal	N_{In} (cm^{-3})	N_D (cm^{-3})
A	1×10^{17}	3.0×10^{17}
B	1×10^{18}	1.2×10^{18}
C	5×10^{18}	3.5×10^{18}

occur. This is obvious from experiment since the energetic position of the donor bound exciton luminescence (I_2) band remains constant. We assume therefore that the ionizantion energy also remains constant. The doping concentration does not generate significant fluctuations of the band potentials. Each donor-electron does not have an independant transition, but instead it has its possible hole states partially filled by earlier decays of other donor electrons. Therefore the statistical problem becomes more complicated but can be treated by a convolution of the time scale.[7] For an indium concentration of 1×10^{18} cm^{-3} no significant deviation between the uncompensated case compared to the exact compensation is observed at short times ($t \leq 10^7$ s). At intermediate times ($10^7 \leq t \leq 10^3$), the reduced hole concentration decreases the recombination rate of an electron so that the exactly compensated curve falls below the partially compensated one once sufficient time has elapsed for about half of the carriers to recombine. For long times, the exact compensated curve is situated above the partially compensated ones because the recombiation which did not take place at intermediate times finally occurs. Here the compensated curves decay as t^{-2}.

2. *Excitonic transitions (region II)*

The inset of Fig. 3 presents the time-integrated luminescence spectrum of an undoped CdS crystal showing the free exciton at 2.5528 eV as well as excitons bound to ionized donors (D^+, X) (the I_3 line), bound to neutral donors (D^0, X) (the I_2 line), and bound to neutral acceptors (A^0, X) (the I_1 line). The main part of Fig. 3 depicts transients of these excitonic transitions, yielding decay times of (980±30) ps for the I_1 line, (300±30) ps for the I_2 line, (50±20) ps for the I_3 line, and (100±20) ps for the free A exciton (X line). The observed rise time τ_{rise}= (100±10) ps of the I_1 and I_2 lines are in good agreement with the decay time of the free exciton. The lifetimes of the bound exciton complexes increase with increasing binding energy, which is confirmed for a large variety of II-VI semiconductors.[23] This trend is in good agreement with theoretical calculations for a pure radiative decay by Rashba and Gurgenishvili[24] (R&G) connecting the bound exciton oscillator strength via the exciton localization with the free exciton oscillator strength per molecule. The lifetime τ (and therefore the oscillator strength f of the complex) is connected with the binding energy E_B as follows:

$$\tau = \frac{1}{f}\frac{3mc^3}{2e^2n\omega^3} \propto E_B^{-3/2} . \quad (3)$$

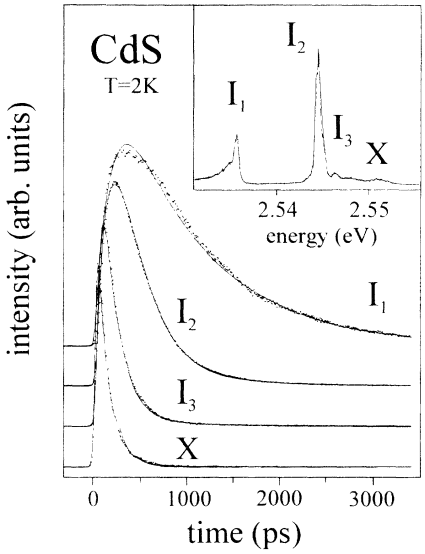

FIG. 3. Transients of an undoped CdS crystal under low excitation densities (I_{exc}=1 kW cm^{-2}). Transients of the free A exciton (X), the (A^0, X) complex (I_1), the (D^0, X) complex (I_2), and the (D^+, X) complex (I_3) are presented. The inset shows the luminescence in the excitonic region. The spectral resolution is responsible for the observed linewidths.

Figure 4 depicts transients of the near-band-gap luminescence for increasing indium concentration, taken at the energy position of the I_2 line in undoped CdS. The crystal with $N_{\text{In}} \approx 10^{17}$ cm^{-3} (curve A in Figs. 1 and 4) reveals spectrally separated luminescence lines I_1 and I_2. The decay times are τ= 100 ps for the I_2 line and τ= 800 ps for the I_1 line, which is significantly shorter than in undoped CdS (Fig. 3). For higher indium concen-

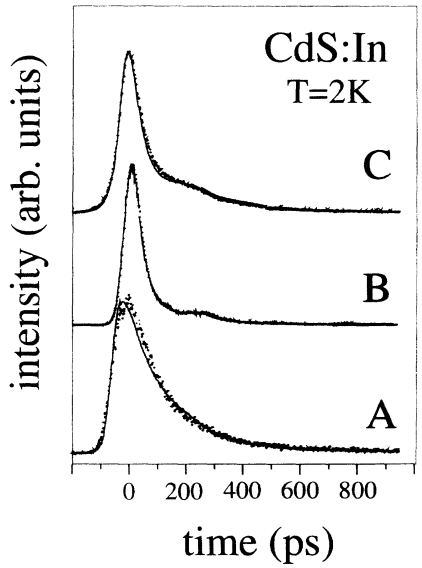

FIG. 4. Transients of CdS:In crystals with indium concentrations below the Mott density for low excitation densities (10 kW cm^{-2}) at the energy position of the I_2 in undoped CdS. The fitted rise and decay times as well as the amplitude ratios are given in the text.

trations A two-exponential decay (τ_1, τ_2) with varying amplitudes (A_1,A_2) is easily fitted to the luminescence transients. At $N_{In}=1\times10^{18}$ cm^{-3} (curve B in Figs. 1 and 4) one gets $\tau_1=$ 50 ps and $\tau_2=$ 200 ps with an amplitude ratio A_1/A_2 of 4. Finally, for $N_{In}=5\times10^{18}$ cm^{-3} (curve C in Figs. 1 and 4) the recombination times decrease to $\tau_1=$ 30 ps and $\tau_2=$ 150 ps with an amplitude ratio A_1/A_2 of 33. It is interesting to notice that the ratio of the amplitude A_1/A_2 of both decay components (τ_1, τ_2) depends on the spectral position and increases with increasing indium concentration. This behavior is valid for the two crystals B and C (Fig. 1).

Figure 5 shows the amplitude ratio of the two decay components (τ_1, τ_2) of the excitonic luminescence band at $N_{In}=1\times10^{18}$ cm^{-3}. With decreasing energy of detection the slower component τ_2 dominates the luminescence dynamics. 15% to 55% of the measured luminescence intensity decays with τ_2. Based on the measured distribution for the decay constants over the whole luminescence band, τ_1 is attributed to the decay of the (D^0,X) complex with an amplitude A_1 and τ_2 to the decay of the (A^0,X) complex with an amplitude A_2. The decay component τ_1 of the broad luminescence band in indium-doped CdS is shorter than the I_2 recombination time in high purity CdS crystals. An increasing indium concentration leads obviously to a reduction of the lifetimes of the excitonic complexes.

In time-integrated luminescence spectra a broadening of the (D^0,X) complex recombination (I_2 line) with increasing donor concentration is observed (Fig. 1). The screening of the Coulomb interaction with increasing donor concentration in CdS:Cl (Ref. 5) leads to a reduction of the binding energy of the exciton-impurity complex, which is equivalent to a reduction of the localization of the exciton. The broadening of the I_2 line can be explained by Coulomb screening of the exciton bound to a neutral donor. An equivalent explanation has to be considered for indium-doped CdS, which is confirmed by the observed luminescence dynamics. Therefore, this picture is in agreement with excitonic recombination mechanisms at indium concentrations below the Mott density.

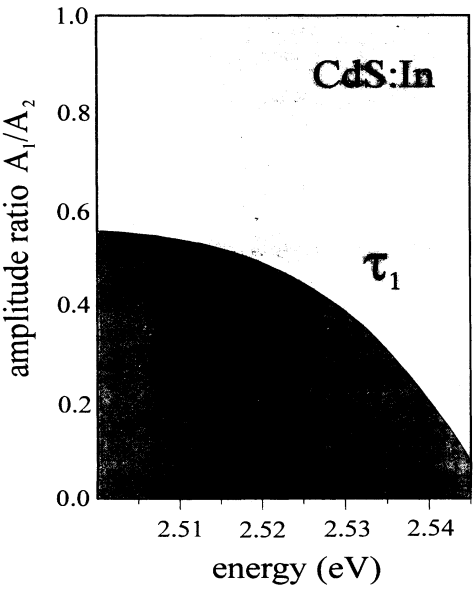

FIG. 5. Amplitude ratio A_1/A_2 for the decay components (τ_1,τ_2) for a crystal with $N_{In}=1\times10^{18}$ cm^{-3} (curve B in Figs. 1 and 4).

The theoretical work of R&G (Ref. 24) yields a simple explanation for the observed increase of the bound exciton transition probability with increasing donor concentration. R&G consider only an isolated impurity center in an ideal crystal without taking into account the interaction of the bound exciton complex with neighboring donor atoms. This becomes important with increasing indium concentration. As a first correction the average distance between neighboring impurity centers is to be taken into account. The spatial screening range at a given doping concentration compared to the Bohr radius of the exciton-impurity complex is a measure for the influence of doping onto the binding energy. The higher the doping concentration, the greater the extension of the Coulomb screening on the donor-exciton binding energy. Therefore, the effective binding energy of the bound exciton complex is lowered and employing Eq. (3) the radiative decay times become shorter, but still bound exciton complexes exist.

Since in CdS:In the number of donors is by far larger than the number of acceptors, the environment of a donor or an acceptor is comparable. The increasing indium concentration affects donors as well as acceptors, therefore both (D^0,X) and (A^0,X) complexes will recombine in shorter times than in undoped CdS samples. The donor-donor or acceptor-donor interaction is similar and the Coulomb screening takes place for acceptor-exciton complexes as well as for donor-exciton complexes.

In undoped CdS crystals decay times τ_2 for the (A^0,X) complex around 1000 ps are measured (Fig. 3). Since the amplitude ratio of A_1/A_2 decreases with increasing doping concentration, the (A^0,X) luminescence remains obviously constant or decreases much slower than the (D^0,X) complex. The strong broadening of the I_2 line with increasing doping gives place to a dominating luminescence band, preventing the measurement of the isolated I_1 line. We observe this behavior for all the samples with indium concentrations below the Mott density. The inhomogeneous line broadening due to spatially inhomogeneous doping throughout the sample underlines this interpretation of the bound exciton decay.

A relation between the indium doping concentration and the observed decay times is obvious. Nevertheless no model to calculate the doping concentration from these results is available yet.

3. Non-k-conserving band-to-band recombination (region III)

The crossover of the luminescence from excitonic- to non-k-conserving band-to-band recombination for indium concentrations around the Mott density can be seen from time integrated spectra (Fig. 1). However, the changes of the dynamical behavior (Fig. 6) for these concentrations are more pronounced. Both donor and acceptor states no longer exist. The band structure of the semiconductor is renormalized and the indium impurities

form a part of the conduction band. The renormalized nonparabolic band and the Fermi level are the parameters to determine the transition energy of the expected luminescence. Conductivity and hall measurements show that our crystals have a high conductivity and a high mobility for electrons. This behavior shows that our crystals are highly uncompensated and therefore the DAP luminescence vanishes for high indium concentrations and the electronic dynamics changes drastically. Now the recombination of free charge carriers is responsible for the observed luminescence. Since the band-to-band transition probability is smaller than the exciton transition probability, slower decay times are expected. This change is obvious from time-resolved measurements below and above the Mott density.

Figure 6 represents transients of non-k-conserving band-to-band transitions for indium concentrations above the Mott density in a logarithmic plot. The transition from localized excitonic states to a degenerated semiconductor is clearly resolved comparing the dynamical behavior of the near-band-gap luminescence above and below (see Fig. 4) the Mott density. As will be discussed below multiexponential fits are no longer suitable to describe the decay. Nevertheless, exponential fits of the early parts of the transients show a general trend with increasing indum concentration. At $N_{\mathrm{In}}= 3\times10^{19}$ cm^{-3} the first decay components τ_1=80 ps indicate a drastically slower decay than in the case of excitonic recombination (τ_1=30 ps) for $N_{\mathrm{In}}=5\times10^{18}$ cm^{-3}. However, with increasing indium concentration τ_1 decreases down to 10 ps.

A simple description in terms of non-k-conserving band-to-band transitions in terms of a two-level or multilevel system fails, since no localized states are involved. A detailed description of these transitions can be given, taking into account the number of occupied states in the excited level and the number of free states in final level. As motivated in Ref. 13, by neglecting the role of acceptor states for the recombination process, the recombination rate is proportional to the concentration of electrons in the conduction band and the concentration of holes in the valence band. The indium doping leads to a partly filled metal-like conduction band. The concentration of doping-generated electrons is given by $n_0=N_D-N_A$. The incoming laser pulse creates additional electrons $n_{\mathrm{exc}}(t)$ as well as holes. The optical-generated electrons fill the empty states in the conduction band at large energies and k vectors. The holes are situated near the valence-band maximum and therefore have k vectors nearly zero per cm^{-3} of electrons n_0 which are generated by doping and have a relatively small mean value of the k vector and may be defined as α_1^{CV}. The recombination constant for electrons $n_{\mathrm{exc}}(t)$ with large k vectors is given by α_2^{CV} in cm^{-3}. With I_{exc} the excitation density per cm^2, $h\nu_{\mathrm{exc}}$, the photon energy, and V_{exc}, the excited volume of the crystal, one gets

$$\frac{dn_{\mathrm{exc}}(t)}{dt} = -\alpha_1^{CV}\, n_0\, n_{\mathrm{exc}}(t) - \alpha_2^{CV}\, n_{\mathrm{exc}}^2(t)\ , \qquad (4)$$

$$n_{\mathrm{exc}}(t=0) = \frac{I_{\mathrm{exc}}}{h\nu_{\mathrm{exc}} V_{\mathrm{exc}}}\ ,$$

with the solution

$$\frac{n_{\mathrm{exc}}(t)}{n_{\mathrm{exc}}(t=0)} = \frac{\frac{\alpha_1^{CV} n_0}{\alpha_2^{CV} n_{\mathrm{exc}}(t=0)}}{-1+\left[1+\frac{\alpha_1^{CV} n_0}{\alpha_2^{CV} n_{\mathrm{exc}}(t=0)}\right]\exp\left[\frac{t}{\Theta}\right]}\ , \qquad (5)$$

$$\Theta = \frac{1}{\alpha_1^{CV} n_0}$$

and the luminescence intensity at time t is given by

$$\frac{I(t)}{I(t=0)} = \frac{d}{dt}\left(\frac{n_{\mathrm{exc}(t)}}{n_{\mathrm{exc}}(t=0)}\right)\ . \qquad (6)$$

Equation (6) describes a nonexponential decay depending on the ratio of the doping- to the photogenerated transitions rates $\alpha_1^{CV}\ n_0/\ \alpha_2^{CV}\ n_{\mathrm{exc}}(t=0)$ and Θ. The resulting fits $I(t)/I(t=0)$ are in good agreement with the measured data (Figs. 6 and 7). The parameter Θ has the dimension of time and influences the bending of the curve. The fitted value gives the product $(\alpha_1^{CV} n_0)^{-1}$. We observe with increasing indium concentration decreasing values for Θ. This is in accordance with an increasing n_0, admitting an almost equal transition constant α_1^{CV} for all investigated crystals. To obtain the transition constant α_1^{CV} an independent determination of the doping concentration n_0 for one crystal is then necessary. Hall measurements for the crystal D in Fig. 1 by Broser *et al.*[12] reported a mobility of 160 cm^2 V^{-1} s^{-1} and a calculated carrier concentration of $n_0=5\times10^{19}$ cm^{-3}. With this carrier concentration and the fitted time constant Θ, α_1^{CV} is determined to $[a_{CV}= (7.4\pm1.0)\times10^{-11}$ s^{-1} cm^{-3}. Calculated values for Θ and $\alpha_1^{CV}\ n_0/\alpha_2^{CV}\ n_{\mathrm{exc}}(t=0)$ are given in Table II. The values of n_0 are in good agreement with the concentrations deduced from the growth

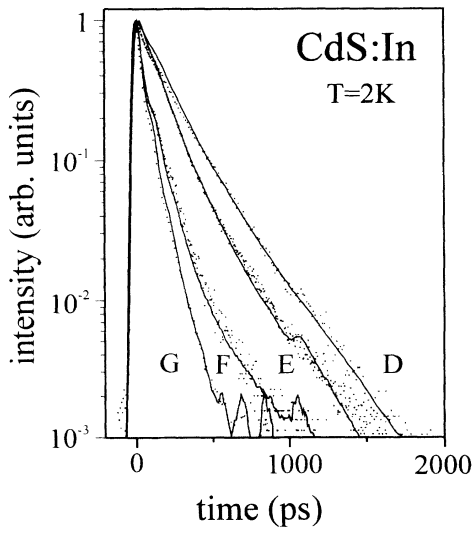

FIG. 6. Transients of the non-k-conserving band-to-band luminescence for CdS:In (dots) at 10 kW cm^{-2} fitted using Eq. (5) described in the text. The parameters are given in Table II.

TABLE II. Fitted values according to Eq. (5) for crystals $D-G$ (see Fig. 1).

Crystal	$\frac{\alpha_2^{CV}}{\alpha_1^{CV}}$	$\frac{n_0}{n_{exc}(0)}$	Θ (ps)	n_0 (cm^{-3})	N_{In} (cm^{-3})
D	1×10^3	1×10^3	270	5.0×10^{19}	1×10^{19}
E	2×10^3	1×10^3	230	5.9×10^{19}	5×10^{19}
F	6×10^3	1×10^3	190	7.1×10^{19}	7×10^{19}
G	1×10^4	1×10^3	120	1.13×10^{20}	1×10^{20}

conditions for all the samples with indium concentrations above the Mott density. The function $n_{exc}(t)$ is directly correlated to the density of photogenerated electrons or holes and $n_{exc}(t=0)$ is the concentration of electron-hole pairs generated by the incoming laser pulse. The ratio $\alpha_1^{CV} n_0/\alpha_2^{CV} n_{exc}(t=0)$ is directly determined by the experimental conditions.

For low excitation densities values of the ratio $\alpha_1^{CV} n_0/\alpha_2^{CV} n_{exc}(t=0)$ in the order of magnitude one are obtained. This seems to be in conflict with the experimental situation, since n_0 is certainly larger than $n_{exc}(t=0)$. Under the assumption of a strong variation of the recombination constants α_1^{CV} and α_2^{CV} with a k vector for band-to-band transitions, an explanation can be given. The majority of the doping-induced electrons is situated at small energies, and therefore the mean value of the k vectors in the conduction band is small, while the photogenerated electrons are created in a small region near the Fermi level with large k vectors. Optical transitions of these electrons are detected by our experimental setup in a small energy range for highest values of the k vectors. A further observation is that the smaller the energy of detection, the longer the detected decay of the luminescence. This luminescence results from the recombination of electrons, which have reduced k vectors and thus smaller transition constants compared to those transitions at higher energies. An additional effect, which changes the fitted recombination constants, might arise from the fact that our crystals are not uniformly indium doped. Assuming a strong reabsorption of luminescence light in highly doped regions, the detected light steems from lower doped regions compared to the average doping concentration. Measurements of the conductivity will give in contrast only values for the average doping concentration.

4. High excitation densities

High excitation densities influence strongly the luminescence dynamics observed for CdS:In at the investigated indium concentrations. Exciton, DAP, and non-k-conserving band-to-band recombination processes become faster, indicating an influence of high excitation densities on the recombination dynamics. The creation of an electron-hole plasma by high excitation densities in addition of a dense electron gas due to the indium doping changes further the recombination dynamics. At intensities of 0.5 GW cm^{-2}, approximately 2×10^{11} photons per laser pulse are realized at photon energies of 2.7 eV, which is above the energy of the band gap of CdS:In. The light is absorbed in a thin layer near the surface and therefore concentrations $n_{exc}(t=0)$ of charge carriers of about 5×10^{18} cm^{-3} are obtained. Now the density of photoexcited carriers, i.e., electrons and holes, is of the same order of magnitude as the doping-induced electron density. Typical high excitation phenomena such as biexciton or exciton-exciton–collision luminescence are not observed in indium-doped CdS crystals in spite of the high excitation densities. Diffusion of the charge carriers is obviously very efficient and reduces in extremely short times the concentration of photogenerated electrons and holes near the surface. The diffusion constants are additionally different for a doping-induced dense electron gas and a photogenerated electron-hole plasma.

Figure 7 shows decay times obtained by exponential fits of the early parts of the excitonic or band-to-band luminescence transients, respectively, for the whole range of indium concentrations available as well as under different excitation conditions. Although exponential fits are not adequate in the case of non-k-conserving band-to-band transitions, they permit us to discuss doping-induced changes of the recombination dynamics. The radiative lifetime of the exciton luminescence below the Mott density, composed of the sum of (D^0,X) and (A^0,X) decay times with varying amplitude ratio, becomes shorter for all the measured samples under high excitation conditions. The interactions of bound exciton complexes increases and leads to smaller effective binding energies. As mentioned before, the I_2 line decays in (300±30) ps in undoped CdS under low excitation conditions. At 500 MW cm^{-2}, $\tau=$ 80 ps for the I_2 line is observed for $N_{In}=1\times10^{17}$ cm^{-3}. The shortest decay time of $\tau=$ 15 ps is measured at $N_{In}=5\times10^{18}$ cm^{-3} (curve C in Fig. 1). The crossover from excitonic to band-to-band recombination at the Mott density, i.e., the formation of a degenerated semiconductor, is reached under high excitation

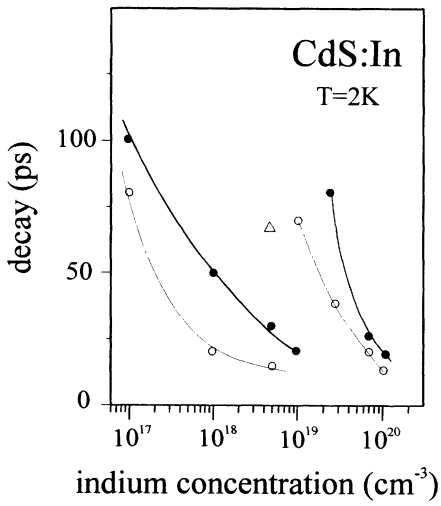

FIG. 7. Exponential fits of the early parts of the near-band-gap luminescence transients of CdS:In. Filled circles show data for 10 kW cm^{-2}, open circles show data for 500 MW cm^{-2}, and the triangle shows data for 1 GW cm^{-2} excitation density.

densities at lower doping concentrations than for low excitation densities and is well represented by exponential fits. An additional increase of the excitation density (triangle in Fig. 7) shifts this crossover to smaller indium concentrations.

As visible from Fig. 7 longer decay times of the luminescence above the Mott density are observed, which are attributed to non-k-conserving band-to-band recombination. Under high excitation conditions, i.e., 500 MW cm^{-2}, this luminescence again becomes faster. Additionally, this type of luminescence is observed at lower indium concentrations. The luminescence decay changes drastically for crystals just below and above the Mott density at low excitation densities. In the crossover region exciton and band-to-band transitions are involved and a combination of both recombination processes is measured in the decay times. Crystals just below the Mott density show under low excitation densities excitonic luminescence whereas under high excitation densities band-to-band luminescence is observed. Actually, the sum of photo-induced and doping-induced carriers is responsible for the type of recombination kinetics observed.

Under high excitation densities the crystals shown in Fig. 6 exhibit transients with highly bimolecular recombination characteristics. Using Eq. (6) to fit, the ratio $\alpha_1^{CV} n_0/\alpha_2^{CV} n_{\mathrm{exc}}(t=0)$ is obtained on the order of 0.5. Therefore, a significant difference for the recombination probabilities α_1^{CV} and α_2^{CV} could not be determined because of the relative small changes of the luminescence dynamics between low and high excitation densities. High excitation densities are realized in experiment in a spatially small region. The electron-hole plasma is generated in a thin layer and the diffusion reduces very effectively this concentration in times smaller than 1 ps. Therefore, the detected light must not be emitted from highly excited regions only, low excitation density luminescence may dominate by intensity. In principle, with Θ fitted to the transients for high excitation densities and the concentration n_0 deduced for low excitation densities, $\alpha_1^{CV}(I)$ and then $\alpha_2^{CV}(I)$ could be determined. The fitted values Θ for all investigated crystals are smaller than under low excitation conditions. This indicates an increase of the recombination probability α_1^{CV}, since the doping-generated carrier concentration n_0 remains constant.

Figure 8 gives transients of the band-to-band luminescence for a highly indium-doped CdS crystal with $N_{\mathrm{In}}=3\times10^{19}$ cm^{-3}, which is not shown in Fig. 1, under high and low excitation densities. Under low excitation densities the experimental data are fitted with $\Theta = 220$ ps, which is equivalent to a carrier concentration of $n_0 = 6.1\times10^{19}$ cm^{-3}. A ratio of $\alpha_1^{CV} n_0/\alpha_2^{CV} n_{\mathrm{exc}}(t=0) = 1500$ is used, indicating that the luminescence decay is nearly exponential. The same recombination constants can be used in this case. Under high excitation densities the density of opticallly generated electrons is in the same order of magnitude as doping-generated carriers. The concentration of holes is significantly increased. Now, high excitation phenomena become possible, leading to a shortening of the luminescence decay. $\Theta = 45$ ps has to be used to fit the transient. The band-to-band

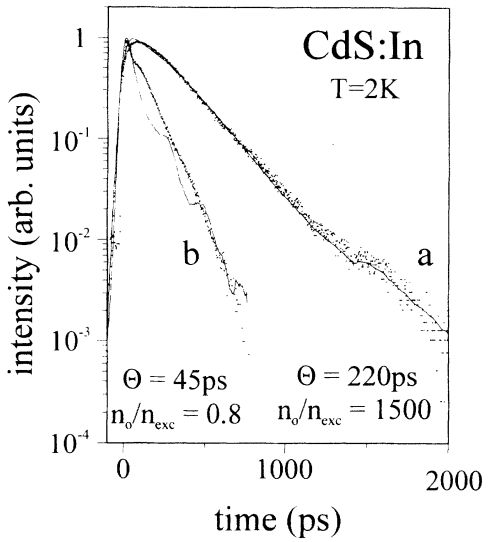

FIG. 8. Transients for CdS:In with $N_{\mathrm{In}}=3\times10^{19}$ cm^{-3} for (a) low (10 kW cm^{-2}) and (b) high excitation (500 MW cm^{-2}) densities.

transition probability α_1^{CV} changes obviously under high excitation conditions. The transient is fitted with a ratio $n_0/n_{\mathrm{exc}}(t=0) = 0.8$ and $\alpha_2^{CV}/\alpha_1^{CV}=1$. Bimolecular recombination dynamics are characteristic for the measured transients. This crystal is obviously different compared to the rest of samples. From the yellow color one concludes that this crystal seems to be highly compensated, whereas the other samples are dark brown to black and similiar in conductivity (as crystal D) with a conductivity of 150–200 cm^2 V^{-1} s^{-1}.

Hall measurements are difficult to fulfill, i.e., the influence of the contacts and of the conduction through the whole volume or through a small layer near the surface is extreme on the experimental data. Time-resolved photoluminescence gives with moderate expense reliable data for high impurity concentrations.

Figure 9 shows time-delayed luminescence spectra of the crystal with $N_{\mathrm{In}}= 5\times10^{18}$ cm^{-3} (curve C of Fig. 1) excited with 1 GW cm^{-2} at 2.7 eV. The known "blue" excitonic luminescence band (Fig. 1), is dominated by an additional luminescence attributed to stimulated emission due to electron-hole plasma luminescence.[20] Gain measurements show amplification factors of 300–800 cm^{-1} (Ref. 14) for this sample under ns excitation. We report here detailed measurements of that luminescence with high temporal resolution in the ps time domain. An exponential fit of the early part of the luminescence transient reveals $\tau= 100$ ps (triangle in Fig. 8). The number of photo-excited carriers is obviously high enough to cross the Mott density. The measured decay behavior is typical for band-to-band transitions.

The measured decay time for the stimulated emission (Fig. 10 curve 2) decays exponentially within $\tau= 80$ ps. This is faster than the luminescence underneath (see Fig. 10 curves 1 and 3). Therefore, we assume that the main part of the observed luminescence is due to the radiative decay of an electron-hole plasma. The transition from an electron-hole gas to a condensed system is lim-

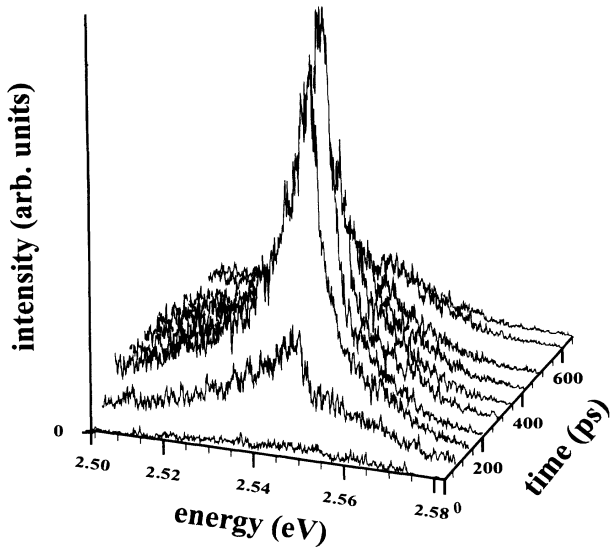

FIG. 9. Time-delayed luminescence spectra of a CdS:In crystal with $N_{In}=5\times10^{18}$ cm^{-3} at T=2 K and an excitation density of 1 GW cm^{-2}. An additional high excitation band is visible at 2.54 eV.

ited by the cooling time of electron and holes, excitons or biexcitons, respectively during their radiant lifetimes. In direct-gap semiconductors such as CdS it is difficult to obtain a condensation of excitons because of the strong exciton-photon coupling, i.e., the polariton effect prevents the accumulation of the particles at the bottom of their band. Band-band excitation, on the other hand, creates only hot carriers which do not cool down during their lifetime giving the possibility to make the condensation into electron-hole-droplets. Recent publications of Yoshida and Shionoya[26] and Swoboda *et al.*[27] show that a condensation of a dense electron-hole gas into the liquid phase is not realized in CdS.

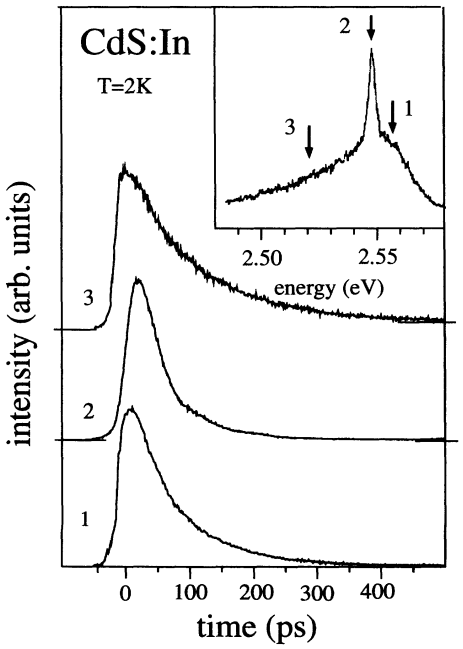

FIG. 10. Transients of a CdS:In crystal with $N_{In}=5\times10^{18}$ cm^{-3} at 1 GW cm^{-2} at different energy positions. The inset shows the corresponding luminescence spectrum.

In undoped CdS crystals the luminescence under highest excitation conditions is attributed to electron-hole-plasma recombination, which decays within 150–200 ps.[25] The exciton lifetime decreases due to an enhancement of the Coulomb screening with increasing indium concentration. Admitting a similar influence of the doping on the recombination dynamics for the plasma as for the exciton lifetime, shorter time constants for the electron-hole plasma are expected for highly indium-doped CdS. Obviously, a strong doping-induced background of electrons reduces effectively the radiative lifetime of an electron-hole plasma.

IV. CONCLUSION

The dynamical behavior of the luminescence in semiconductors is one of the fundamental keys to the understanding of all electronic processes. A fast and reliable method to determine the doping density are time-resolved luminescence measurements. The decay of the donor-acceptor-pair recombination reveals information on doping concentrations and on compensation mechanisms for concentrations below the Mott density. Using the statistical theory of Thomas *et al.*,[7] we have determined the doping concentration of indium in CdS with high accuracy. These values are in good agreement with data of Hall measurements, of atomic absorption spectroscopy, and with values deduced from the growth conditions. Compensation effects can be neglected since the excess concentration of donors is at least one order of magnitude higher than that of acceptors. The role of Coulomb screening effects on exciton-impurity interaction, proposed by Hanamura,[5] is also investigated. No line shift is observed with increasing indium concentration below the Mott density, in contrast to the well known case of CdS:Cl. The influence of doping on the localization of the electron at the donor is observed via the bound exciton lifetimes. Both the (D^0,X) and the (A^0,X) complex (τ_1,τ_2) contribute to the decay of the luminescence. A varying amplitude ratio A_1/A_2 of the corresponding decay components (τ_1,τ_2) throughout the excitonic luminescence band is observed. Indium concentrations above the Mott density (samples with $N_{In} \geq 5\times10^{18}$ cm^{-3}) permits us to study the changes in the recombination dynamics around the semiconductor-metal phase transition. The formation of impurity bands out of isolated levels is directly shown in the dynamical behavior as well as by the energy position of the luminescence band far above the band gap of undoped CdS crystals. Here, non-k-conserving band-to-band transitions characterize the decay times. Calculations on the basis of a model involving the number of occupied states in the conduction band and the number of empty states in the valence band give reasonably good fits of the experimental data. The fit parameters permit us to determine the doping level of donors in CdS:In for concentrations higher than the Mott density. For the investigated concentra-

tion regime of indium time-resolved measurements are a tool to identify the processes involved and to determine the electronically active indium concentration as long as light is emitted from the sample. This method should work in any heavily doped semiconductor.

ACKNOWLEDGMENTS

The authors wish to thank Dr. R. Broser for supplying the crystals. This work was partly supported by the Deutsche Forschungsgemeischaft and the Siemens AG.

[1]J.M. DePuydt, M.A. Haase, H. Cheng, and J.E. Potts, Appl. Phys. Lett. **55**, 1103 (1989).
[2]H. Kukimoto, S. Shionoya, S. Toyotomi, and K. Morigaki, J. Phys. Soc. Jpn. **28**, 110 (1970).
[3]M.D. Moin, G.S. Pekar, and E.A. Salkov, Fiz. Tekh. Poluprovadn. **8**, 202 (1974) [Sov. Phys. Semicond. **8**, 132 (1974)].
[4]S.M. Girvin, Phys. Rev. B **17**, 1877 (1978).
[5]E. Hanamura, J. Phys. Soc. Jpn. **28**, 120 (1970).
[6]K. Colbow, Phys. Rev. **141**, 742 (1966).
[7]D.G. Thomas, J.J. Hopfield, and W.M. Augustyniak, Phys. Rev. **140**, A202 (1965).
[8]S. Geschwind and R. Romestain, in *Light Scattering in Solids IV*, edited by M. Cardona and G. Guentherod, Topics in Applied Physics Vol. 54 (Springer, Berlin, 1984), p. 166.
[9]E.O. Kane, Phys. Rev. **131**, 1532 (1963).
[10]U. Neukirch, I. Broser, and R. Rass, Phys. Status Solidi B **159**, 432 (1990).
[11]U. Neukirch, I. Broser, and R. Rass, J. Cryst. Growth **101**, 743 (1990).
[12]I. Broser, R. Broser, and E. Birkicht, J. Cryst. Growth **101**, 497 (1990).
[13]Ch. Fricke, U. Neukirch, R. Heitz, A. Hoffmann, and I. Broser, J. Cryst. Growth **117**, 783 (1992).
[14]I. Broser and R. Broser-Warminsky, Dtsch. Patentamt Patentschr. No. 814, 193 (1950).
[15]K. Nassau, C.H. Henry, and J.W. Shriever, in *Proceedings of the Tenth International Conference on the Physics of Semiconductors, Cambridge, MA, 1970,* edited by S. P. Keller, J. C. Hensel, and F. Stern (United States Atomic Energy Commission, Division of Technical Information, 1970), p. 629.
[16]N.F. Mott and J.H. Davies, Philos. Mag. B **42**, 845 (1980).
[17]S. Toyotomi and K. Morigaki, J. Phys. Soc. Jpn. **25**, 807 (1968).
[18]S.M. Girvin, Phys. Rev. B **17**, 1877 (1978).
[19]U. Neukirch, I. Broser, and R. Rass, Semicond. Sci. Technol. **6**, A96 (1991).
[20]U. Neukirch, Ph.D. thesis, Technische Universitat Berlin, 1991.
[21]K. Colbow and K. Yuen, Can. J. Phys. **50**, 1518 (1972).
[22]D. G. Thomas, J.J. Hopfield, and K. Colbow, in *Proceedings of the Seventh Interanational Conference on the Physics of Semiconductor, Radiative Recombination, Paris, France, 1964* (Dunod Editeur, Paris, 1964), p. 67.
[23]R. Heitz, Ch. Fricke, A. Hoffmann, and I. Broser, Mater. Sci. Forum **83-87**, 1241 (1992).
[24]E.I. Rashba and G.E. Gurgenishvili, Fiz. Tverd. Tela (Leningrad) **4**, 1095 (1962) [Sov. Phys. Solid State **4**, 807 (1962).
[25]H. Saito and E.O. Goebel, Phys. Rev. B **31**, 2360 (1985).
[26]H. Yoshida and S. Shionoya, Phys. Status Solidi B **115**, 203 (1983).
[27]H.-E. Swoboda, F.A. Majumder, V.G. Lyssenko, C. Klingshirn, and L. Banyai, Z. Phys. B **70**, 341 (1988).

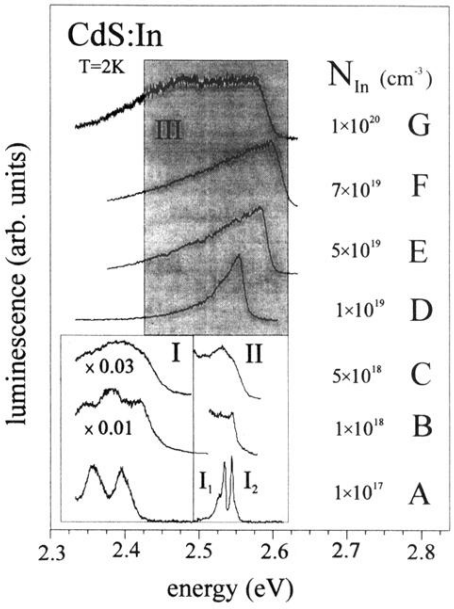

FIG. 1. Luminescence spectra for CdS:In crystals in dependence on the indium concentration for low excitation densities (I_{exc}=10 kW cm^{-2}). Indium concentrations are deduced from growth conditions. The letters *A*–*G*, attributed to each curve, are used for all the figures.

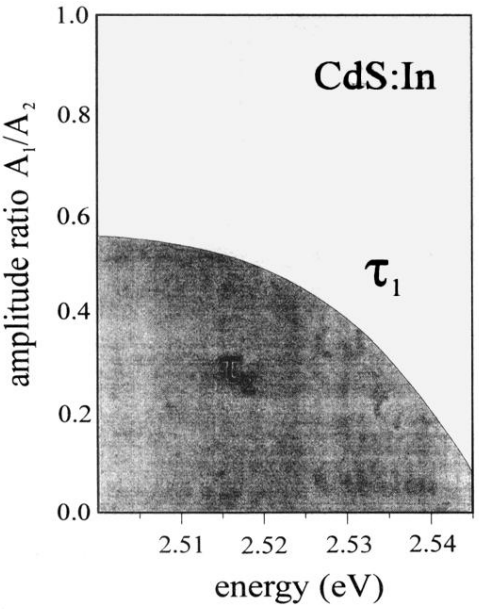

FIG. 5. Amplitude ratio A_1/A_2 for the decay components (τ_1,τ_2) for a crystal with $N_{\mathrm{In}}=1\times10^{18}$ cm^{-3} (curve B in Figs. 1 and 4).